Radboud Universiteit Nijmegen

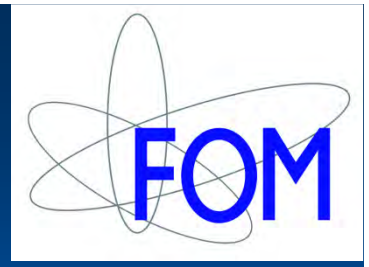

Theory of carbon-based magnetism

Mikhail Katsnelson

Theory of Condensed Matter
Institute for Molecules and Materials
RU

Outline

- *sp* magnetism in general: why it is interesting?

- Defect-induced magnetism in graphene: Lieb theorem, midgap states, and all that

- Zigzag edges, *g*rain boundaries, carbon foam, defected fullerenes...

- Noncollinear magnetism in C_2H and C_2F

- Electron-electron interactions in graphene from first principles

- Effective Hubbard model for carbon materials

Itinerant – electron magnetism: A long-standing problem

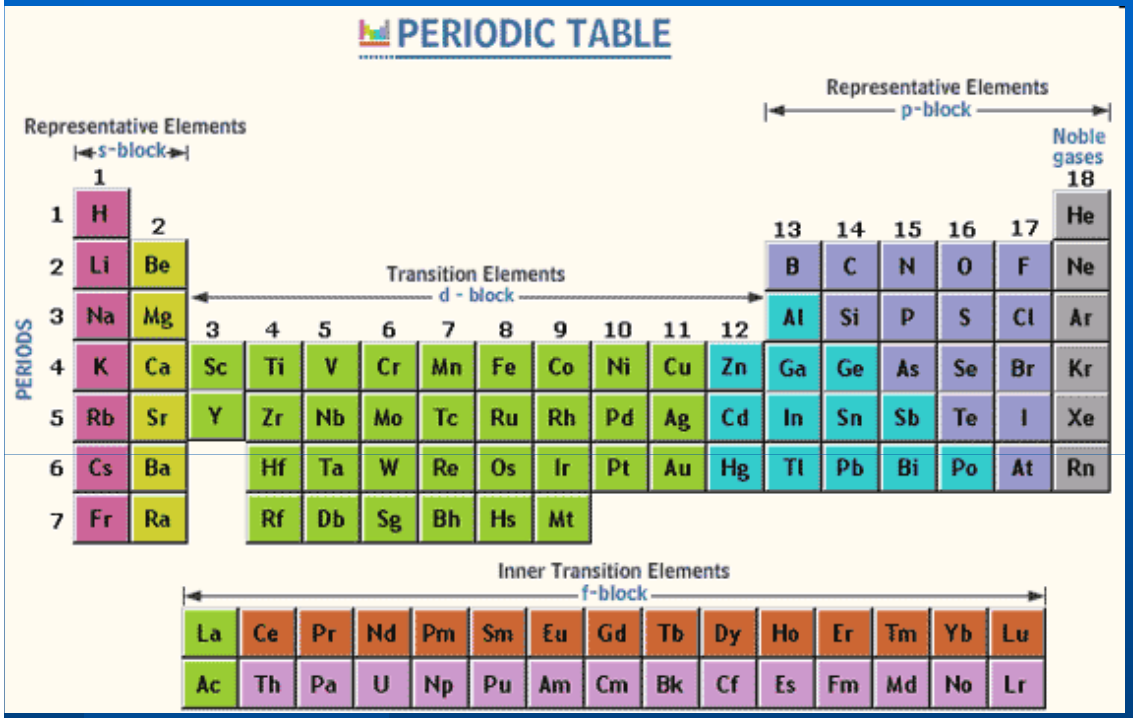

Ferromagnetism of iron is known from ancient times

Iron

Cobalt

Nickel

Problem: coexistence of localized and itinerant behavior

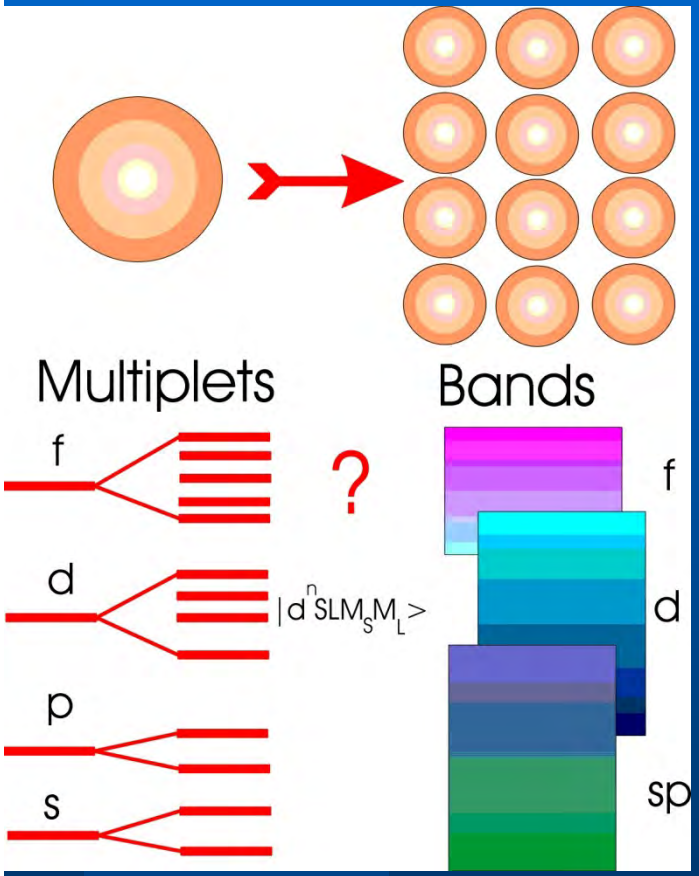

Local magnetic moments do exist above T_C (Curie-Weiss law, spectroscopy, neutrons…)

d electrons are itinerant (FS, chemical bonding, transport…)

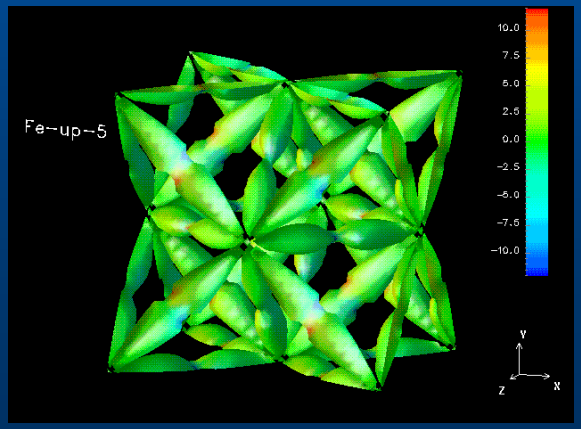

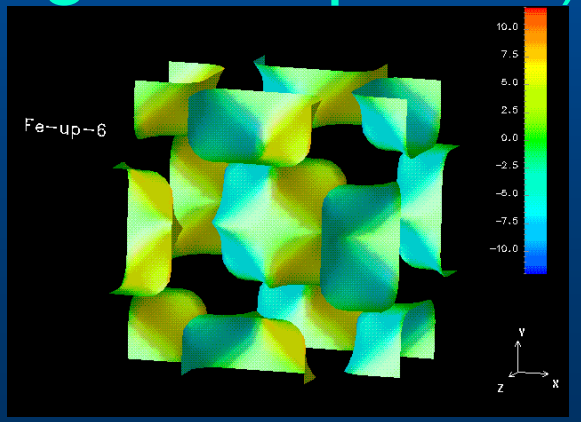

Iron, majority spin FS

4f electrons are normally pure localized but not 3d

Magnetism of *sp* electrons in narrow impurity bands: Model considerations

D.M.Edwards & MIK, JPCM 18, 7209 (2006)

Motivation: "semi-reproducible" magnetism in carbon systems, CaB_6, etc.: defect-related

Theoretically: any essential difference with Fe, Co, Ni itinerant-electron magnetism? Yes!!! Possible way to high Curie temps.

Two main differences

Standard itinerant-electron ferromagnets:

- Strong suppression of Stoner parameter by correlation renormalizations (Kanamori)
- T_C is determined by spin waves rather than Stoner excitations

If Fe would be Stoner magnet it would have $T_C \approx 4000\ K$ (in reality 1043 *K*)

***sp*- electron itinerant electron FMs are Stoner magnets and thus can have much higher T_C than usual dilute magnetic semiconductors**

Stoner criterion

$$I_{\text{eff}} N(E_{\text{F}}) > 1$$

$N(E_{\text{F}})$ is the density of one-electron states

I_{eff} is an on-site interaction parameter

Equation for the Curie temperature:

$$I_{\text{eff}} \int \mathrm{d}E \left(-\frac{\partial f}{\partial E}\right) N(E) = 1$$

***f(E)* Fermi function**

Rectangular band, width W_{imp}:

$$k_{\text{B}} T_{\text{c}} = W_{\text{imp}} / \left[4 \tanh^{-1} \left(W_{\text{imp}} / I_{\text{eff}} n_{\text{imp}}\right)\right]$$

$$k_{\text{B}} T_{\text{c}} < I_{\text{eff}} n_{\text{imp}} / 4$$

Stoner parameter ≈ 1eV
Room-temperature FM:
n_{imp} > 0.01

Kanamori renormalization

T-matrix: $I_{eff} \approx I / [1 + const\ I/W]$

Usually (Fe, Co, Ni…) Stoner criterion satisfies at the border $I_{eff}\, N(E_F) \approx 1.2$.

Impurity bands: T-matrix renormalization can be unusually small due to spectral weight transfer effects

General theory of T-matrix renormalization

Hamiltonian

$$H = H_{\mathrm{t}} + H_{\mathrm{U}}$$

$$H_{\mathrm{t}} = \sum_{\lambda\lambda'\sigma} t_{\lambda\lambda'} c^{\dagger}_{\lambda\sigma} c_{\lambda'\sigma}$$

$$H_{\mathrm{U}} = \tfrac{1}{2} \sum_{\{\lambda_i\}\sigma\sigma'} \left\langle \lambda_1 \lambda_2 \left| v \right| \lambda'_1 \lambda'_2 \right\rangle c^{\dagger}_{\lambda_1\sigma} c^{\dagger}_{\lambda_2\sigma'} c_{\lambda'_2\sigma'} c_{\lambda'_1\sigma}$$

Equation for T-matrix

$$\langle 13 | T^{\sigma\sigma'} (\mathrm{i}\Omega) | 24 \rangle = \langle 13 | v | 24 \rangle - \frac{1}{\beta} \sum_{\omega} \sum_{5678} \langle 13 | v | 57 \rangle \, G^{\sigma}_{56} (\mathrm{i}\omega)$$

$$\times \, G^{\sigma'}_{78} (\mathrm{i}\Omega - \mathrm{i}\omega) \, \langle 68 | T^{\sigma\sigma'} (\mathrm{i}\Omega) | 24 \rangle ,$$

$\omega = (2n + 1)\pi k_{\mathrm{B}} T$ are the Matsubara frequencies

General theory of T-matrix renormalization *II*

Spectral representation:

$$G^{\sigma}_{56}(i\omega) = \int_{-\infty}^{\infty} \mathrm{d}x \, \frac{\rho_{56}(x)}{\mathrm{i}\omega - x}$$

On-site (Hubbard) interaction)

$$\langle 13|T(E)|24\rangle = \langle 13|v|24\rangle + \sum_{5678} \langle 13|v|57\rangle \langle 57|P(E)|68\rangle \langle 68|T(E)|24\rangle$$

$$\langle 57|P(E)|68\rangle = \int_{-\infty}^{\infty} \mathrm{d}x \int_{-\infty}^{\infty} \mathrm{d}y \, \frac{1 - f(x) - f(y)}{E - x - y} \rho_{56}(x) \rho_{78}(y)$$

Conventional itinerant-electron FM vs impurity-band FM

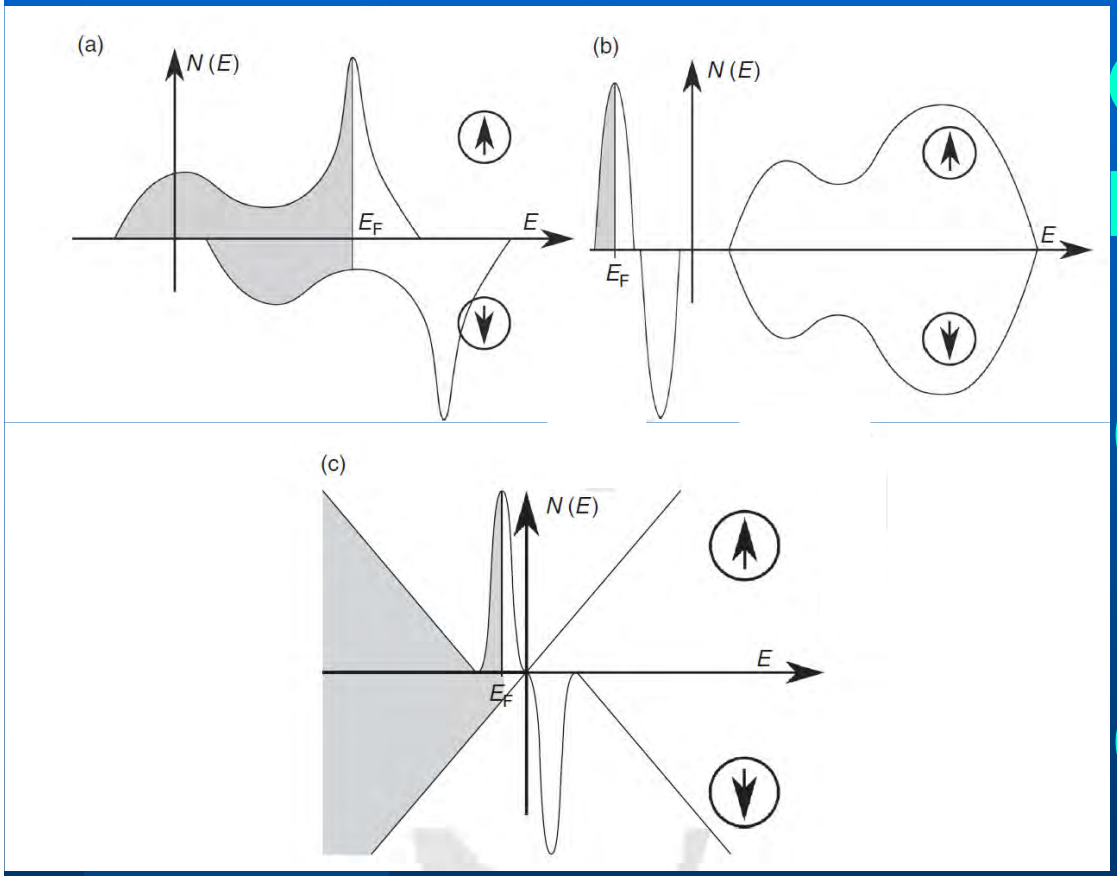

One-band FM, weak polarization

Broad main band (region *I*)

Impurity band (region *II*)

Fig. 12.1. A sketch of the electronic structures for various types of itinerant-electron ferromagnet: (a) the conventional case; (b) and (c) defect-induced half-metallic ferromagnetism in semiconductors and in graphene, respectively.

FM in impurity bands

$$\int_{\mathrm{I}}\int_{\mathrm{I}} \frac{\mathrm{d}x\,\mathrm{d}y}{x+y}\rho\,(x)\,\rho\,(y) \sim \frac{1}{W} Z_{\mathrm{band}}^2,$$

$$\int_{\mathrm{II}}\int_{\mathrm{II}} \frac{\mathrm{d}x\,\mathrm{d}y}{x+y}\rho\,(x)\,\rho\,(y) \sim \frac{1}{W_{\mathrm{imp}}} Z_{\mathrm{imp}}^2,$$

$$\int_{\mathrm{I}}\int_{\mathrm{II}} \frac{\mathrm{d}x\,\mathrm{d}y}{x+y}\rho\,(x)\,\rho\,(y) \sim \frac{1}{W} \ln\left(\frac{W}{W_{\mathrm{imp}}}\right) Z_{\mathrm{band}} Z_{\mathrm{imp}},$$

$$Z_{\mathrm{imp}} = \int_{\mathrm{II}} \mathrm{d}x\;\rho(x),$$

$$Z_{\mathrm{band}} = \int_{\mathrm{I}} \mathrm{d}x\;\rho(x) = 1 - Z_{\mathrm{imp}}$$

Shallow imputities:
Z_{imp} « 1
which suppress suppression of *I*

Magnon stiffness constant in impurity – band FM

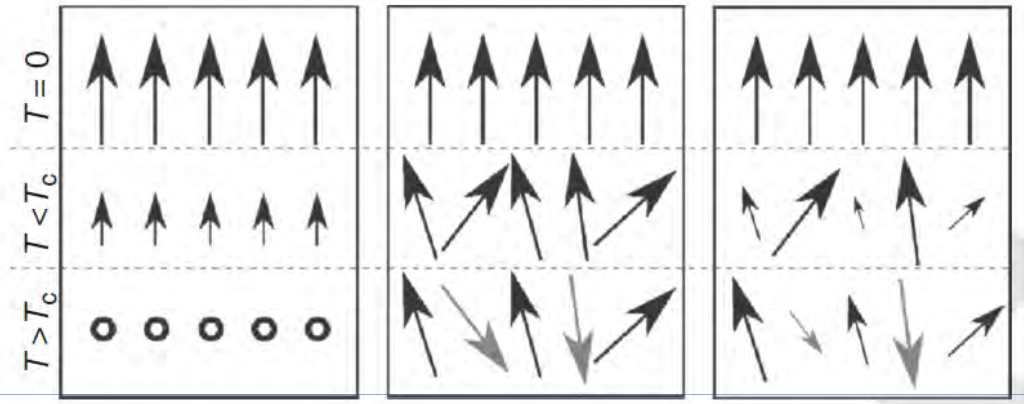

Fig. 12.3. The temperature evolution of ferromagnetic states in the Stoner model (left panel), in the Heisenberg model (middle panel) and in real itinerant-electron ferromagnets (right panel).

Exchange integrals through local rotations

$$c_{im} \rightarrow U(\theta_i, \varphi_i)\, c_{im}$$

where

$$U(\theta, \varphi) = \begin{pmatrix} \cos\theta/2 & \sin\theta/2 \exp(-i\varphi) \\ -\sin\theta/2 \exp(i\varphi) & \cos\theta/2 \end{pmatrix}$$

$$\theta_i = const \text{ and } \varphi_i = \mathbf{qR_i}$$

Magnon stiffness constant in impurity – band FM *II*

$$\delta H = \sum_{ij} Tr_{L\sigma}\left[t_{ij} c_i^{+}\left(U_i^{+} U_j - 1\right) c_j\right] = \delta_1 H + \delta_2 H$$

$$\delta_1 H = \sin^2\frac{\theta}{2}\sum_{k} Tr_{L\sigma}\left[\left(t\left(\mathbf{k}+\mathbf{q}\right) - t\left(\mathbf{k}\right)\right) c_{\mathbf{k}}^{+} c_{\mathbf{k}}\right]$$

$$\delta_2 H = \frac{1}{2}\sin\theta\sum_{ij} Tr_{L}\left[t_{ij} c_{i\downarrow}^{+} c_{j\uparrow}\right]\left(\exp\left(i\mathbf{q}\mathbf{R}_i\right) - \exp\left(i\mathbf{q}\mathbf{R}_j\right)\right)$$

Perturbation theory up to θ^2 with local self-energy (the only approximation)

Magnon stiffness constant in impurity – band FM *III*

$$D = \frac{1}{6\pi\,(n_\uparrow - n_\downarrow)}\,\mathrm{Im}\int_{-\infty}^{E_\mathrm{F}} \mathrm{d}E \sum_{\mathbf{k}} \left[G^{\uparrow}_{\mathbf{k}}(E) - G^{\downarrow}_{\mathbf{k}}(E)\right]^2 |\nabla_{\mathbf{k}}\epsilon\,(\mathbf{k})|^2$$

RPA value of the stiffness constant:

$$D_0 = -\frac{R^2}{6\,(n_\uparrow - n_\downarrow)}\,\langle H_0\rangle = \frac{1}{12}R^2 W$$

Estimation for simplest model, NN hopping

$$D = D_0 + D_1 \simeq \frac{1}{9}\frac{\hbar^2}{2m^*} = \frac{1}{9}D_0$$

no smallness in electron concentration!

Magnon energies are higher than the Fermi energy of electrons!

- **normal itinerant- electron magnets: easier to rotate spins than to change their length**
- ***sp*-magnets: Stoner magnets (after *70 years of existence of the Stoner model a region of applicability was found)***

Vacancies and other sp^3 defects

Lieb theorem: Hubbard model for bipartite lattice

$$\hat{H} = \sum_{ij\sigma} t_{ij} \hat{c}^{+}_{i\sigma} \hat{c}_{j\sigma} + U \sum_{i} \hat{n}_{i\uparrow} \hat{n}_{i\downarrow}$$

$$\hat{t}_{\mathrm{AA}} = \hat{t}_{\mathrm{BB}} = 0$$

NN approx.

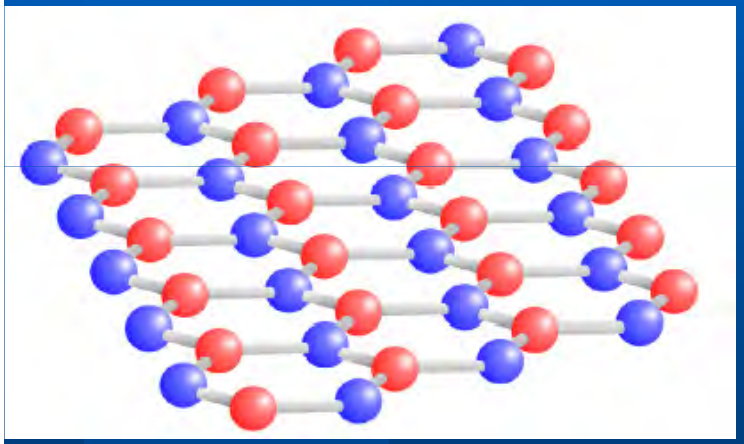

Two equivalent sublattices, A and B (pseudospin)

N_{A} and N_{B} Number of sites in sublattices

The ground state spin: $S = \dfrac{N_{\mathrm{B}} - N_{\mathrm{A}}}{2}$ Lieb, PRL 1989

Vacancies and other sp^3 defects II

- Mid-gap states lead to (local) spin polarization
  - FM exchange in the same sublattice, AFM between A and B
- Hydrogen and other sp^3 defects act very similar to vacancies

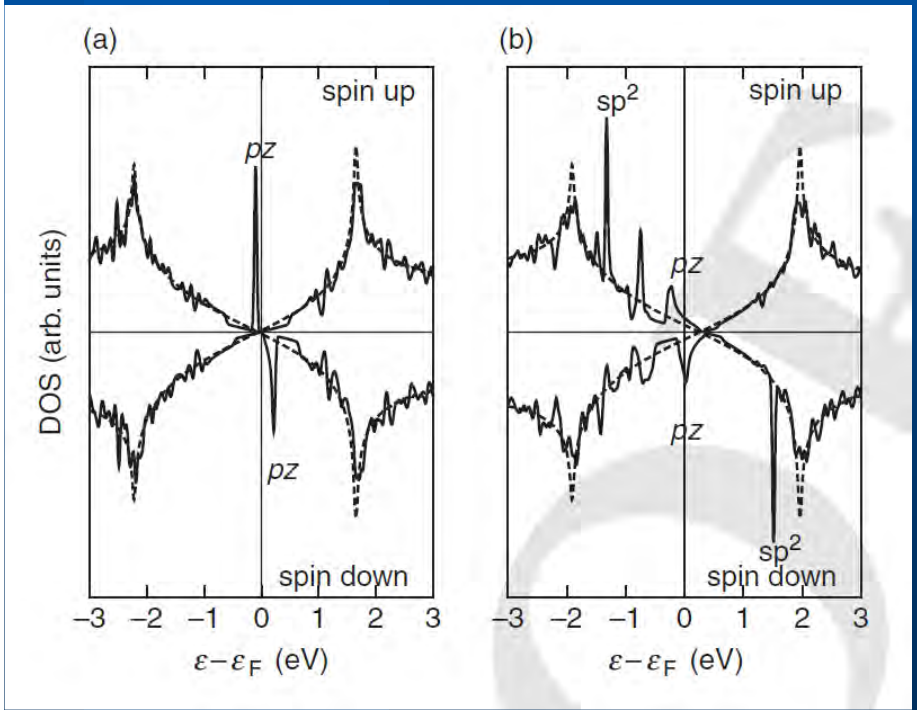

(a) H adatom
(b) Vacancy

Yazyev & Helm, PRB 2007

Vacancies and other sp^3 defects III

Dual origin of defect magnetism in graphene and its reversible switching by molecular doping

R.R Nair[1], I-L Tsai[1], M. Sepioni[1], O. Lehtinen[2], J. Keinonen[2], A.V Krasheninnikov[2,3], A.H Castro Neto[4], M.I Katsnelson[5], A.K Geim[1] & I.V Grigorieva[1]

NATURE COMMUNICATIONS | 4:2010 | DOI: 10.1038/ncomms3010

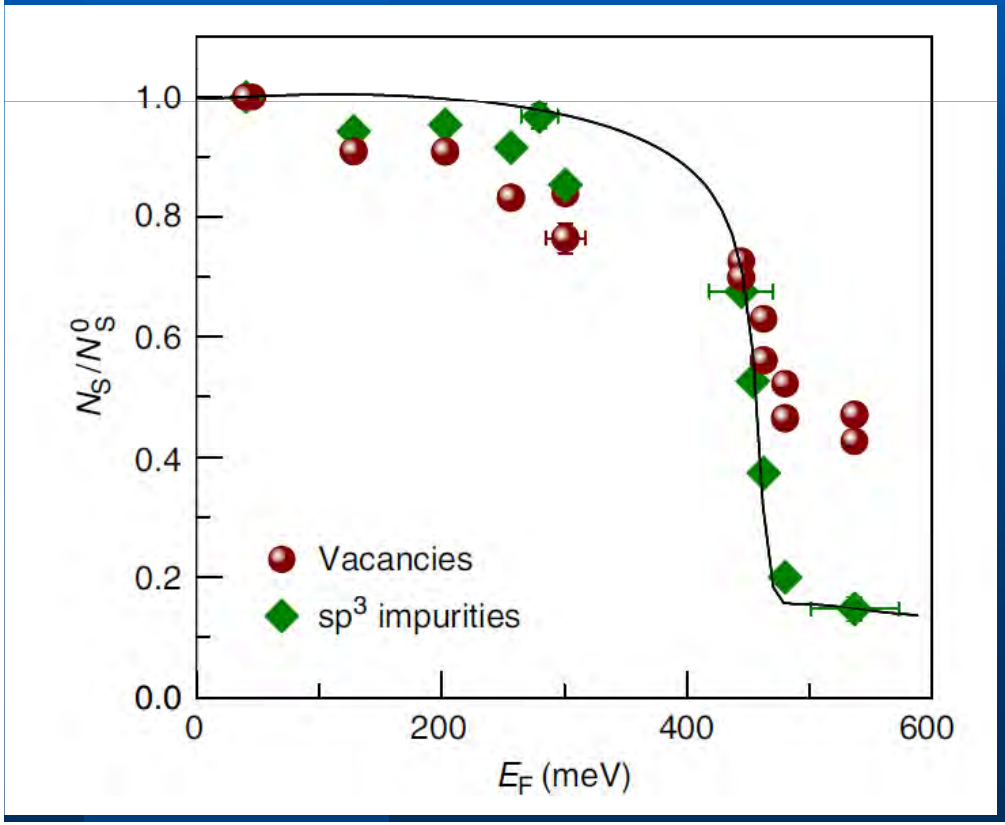

Vacancies: two types of LMM: π (midgap states) and σ (dangling bonds); admolecules: only π

No signs of magnetic order!!!

Polymerized fullerenes

A very controversial issue (experimentally)

D.W. Boukhvalov & MIK, EPJ B 68, 529 (2009)

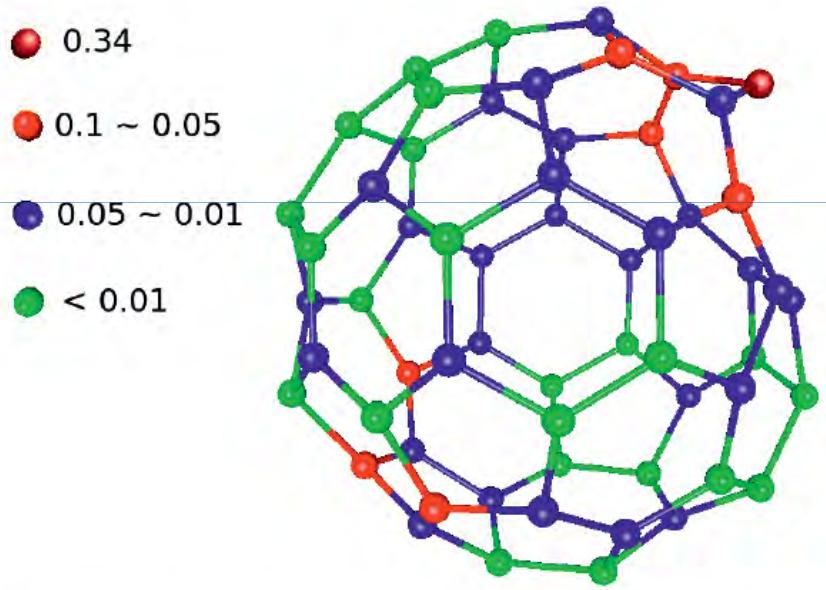

Fig. 4. (Color online) Distribution of magnetic moments in μ_B on C_{60} sphere with single vacancy in rhombohedral phase.

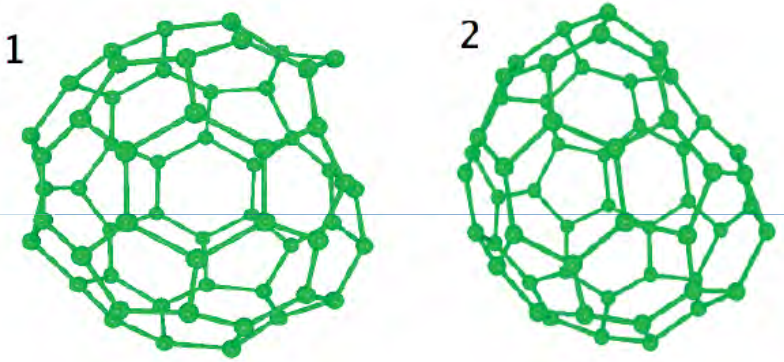

Bivacancy (2) is nonmagnetic and more favourable (2 eV per atom lower)

Single vacancy is magnetic

Magnetism at zigzag edges

Half-metallic graphene nanoribbons

Young-Woo Son[1,2], Marvin L. Cohen[1,2] & Steven G. Louie[1,2]

Nature 444, 347 (2006)

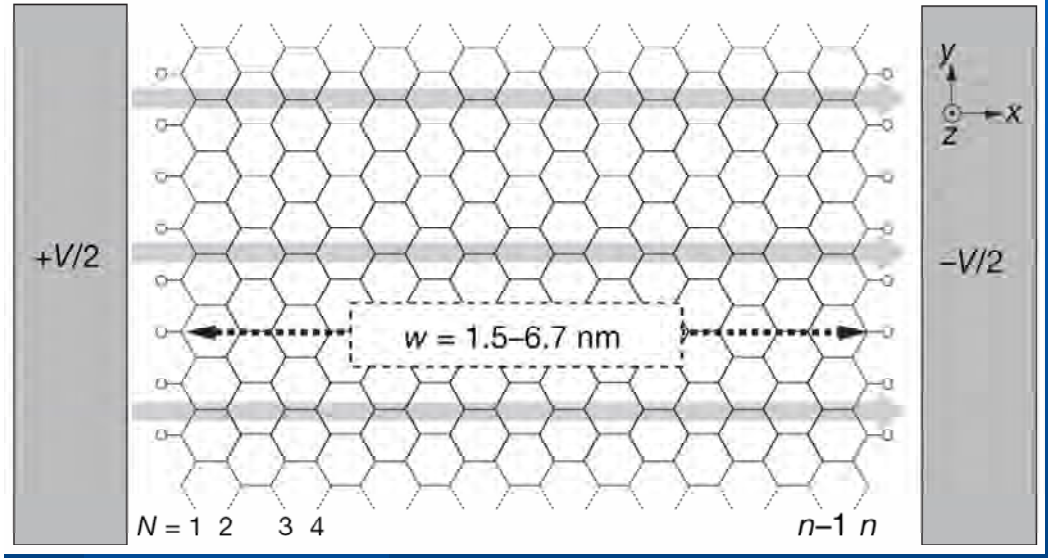

Zigzag edges: midgap states in nonmagnetic case (true in a generic case as well)

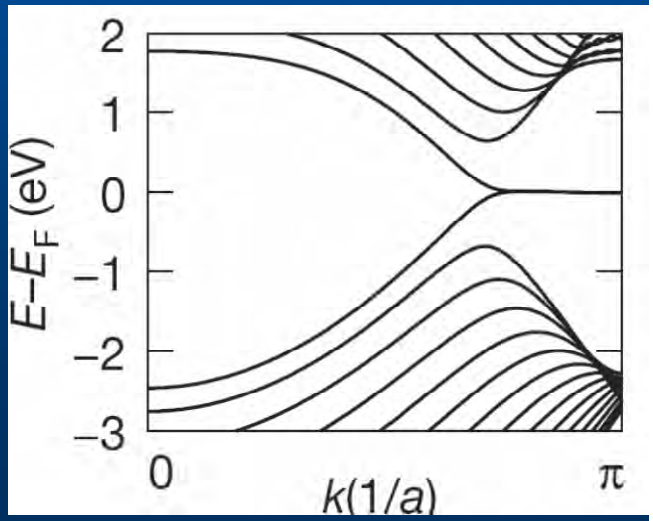

Spin polarization arises

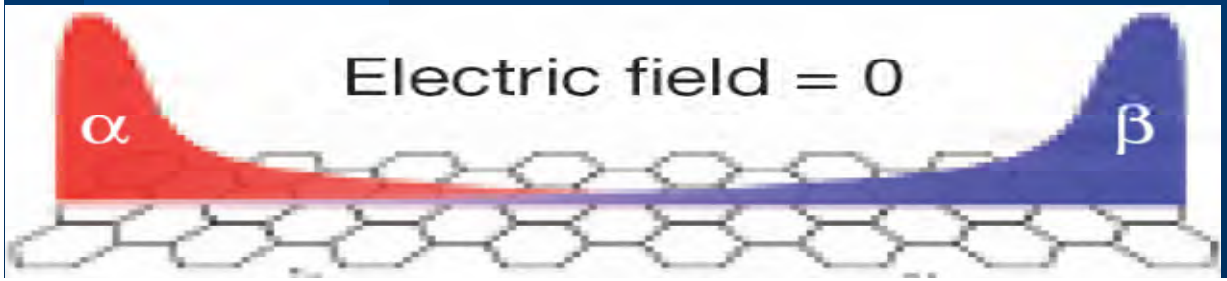

Magnetism at zigzag edges II

1D systems: no magnetic ordering at finite T

Exchange interactions and finite-T magnetism

Yazyev & MIK PRL 100, 047209 (2008)

Energies of transverse (a) and longitudinal (b) configurations, DFT-SIESTA calculations

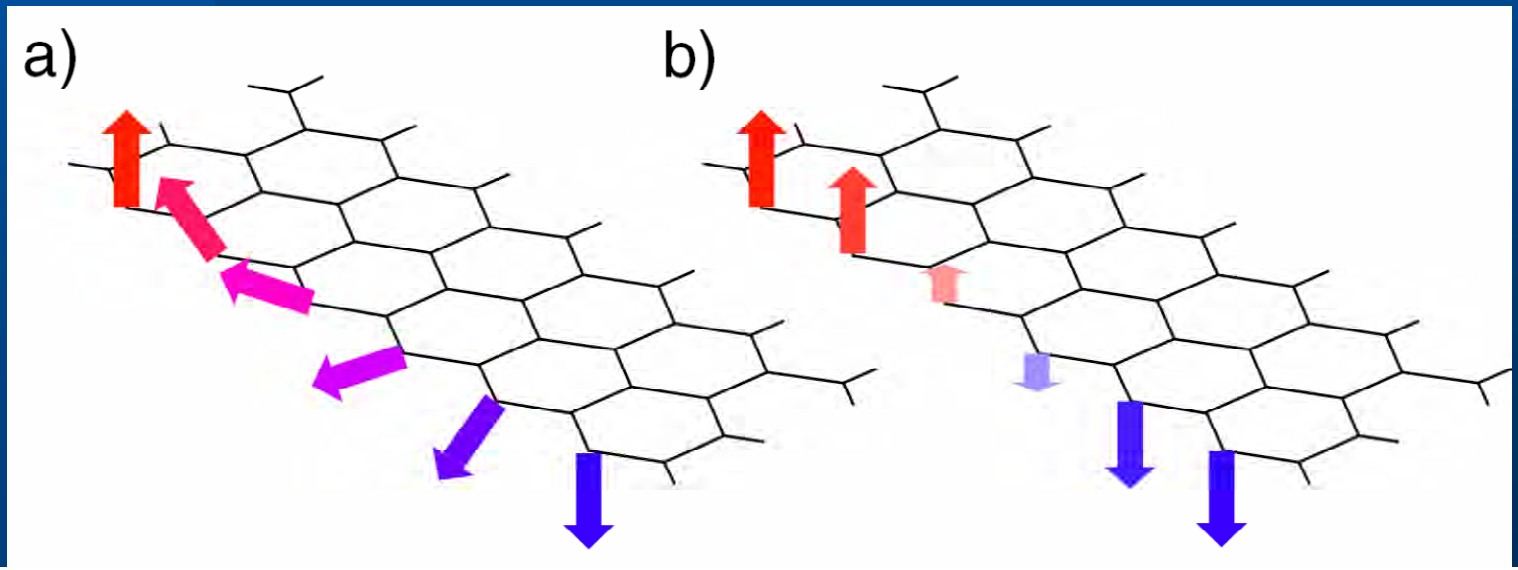

Magnetism at zigzag edges III

A very high spin stiffness constant

$$D = 2100 \text{ meV Å}^2$$

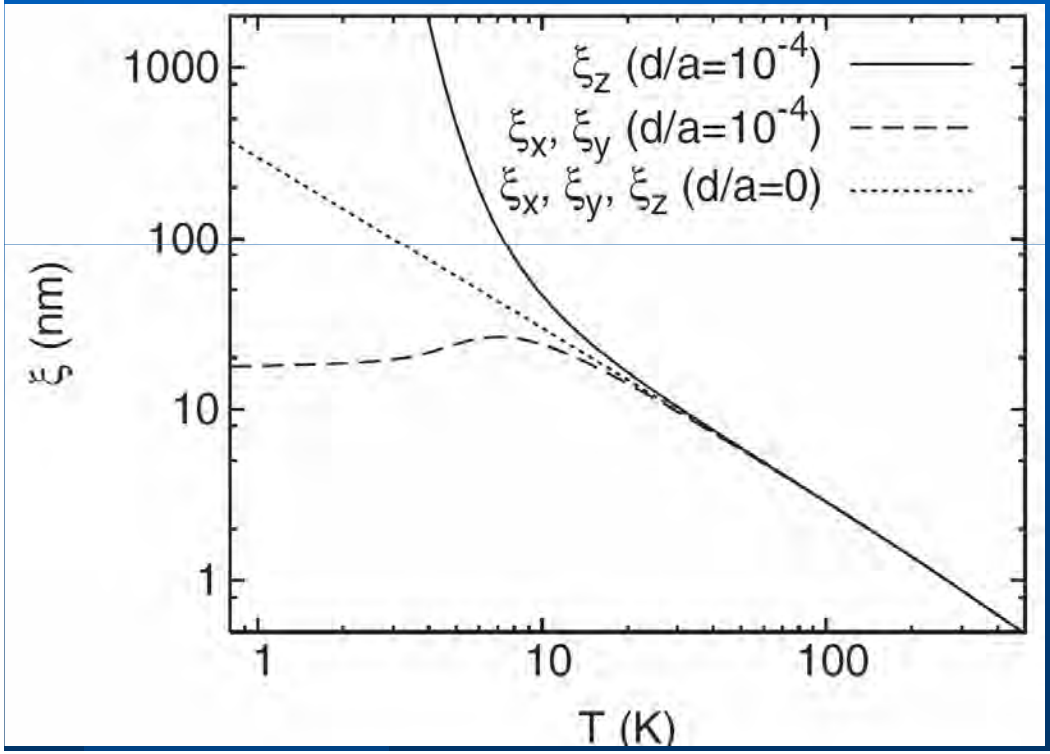

FIG. 3. Correlation lengths of magnetization vector components orthogonal (ξ_z) and parallel (ξ_x, ξ_y) to the graphene plane as a function of temperature T for weakly anisotropic ($d/a = 10^{-4}$) and isotropic ($d/a = 0$) Heisenberg models.

@ RT: Superparamagnetism Enhancement factor 8

Low temperatures: spin coherence at 0.1 μm

Magnetism at zigzag edges IV

Bhandary, Eriksson, Sanyal & MIK, PRB 82, 165405 (2010)

Double-hydrogenated zigzag edges in nanoribbons: still ferromagnetic!

TABLE I. Difference in total energies between the nonmagnetic and ferromagnetic states (ΔE) and the corresponding magnetic moments in the ferromagnetic state. The energy differences and total magnetic moments are quoted for the unit cell whereas the edge moment is for one C atom at the edge.

Width (rows)	ΔE (meV)	Total moment (μ_B)	Edge moment (μ_B)
8	1.63	1.04	0.34
10	5.3	1.23	0.38
15	4.9	1.29	0.39
20	3.81	1.3	0.39

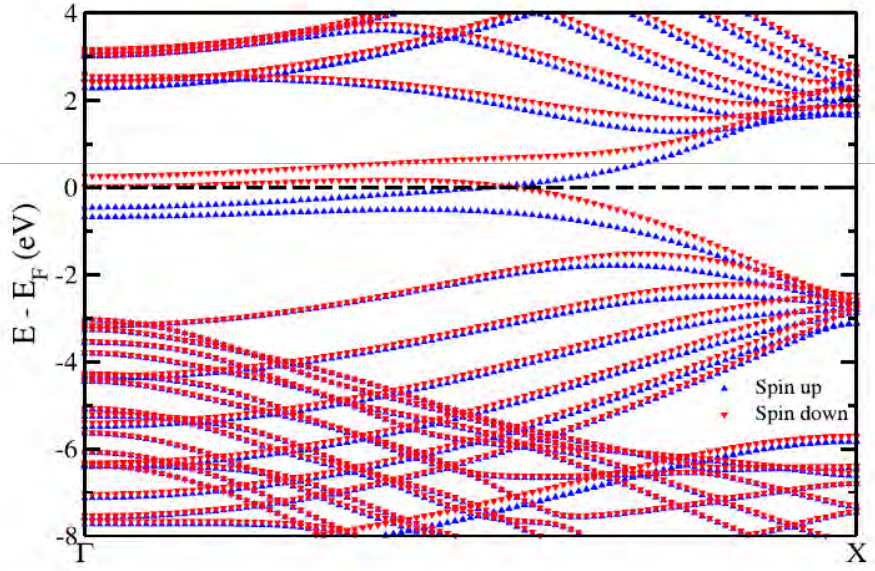

Despite the absence of dangling bonds...

Magnetism at zigzag edges V

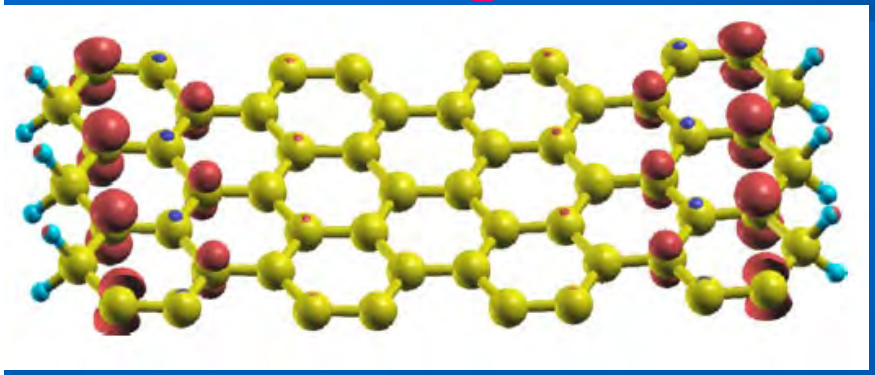

Magnetization density

The model: just cut off double-hydrogenated carbon atoms

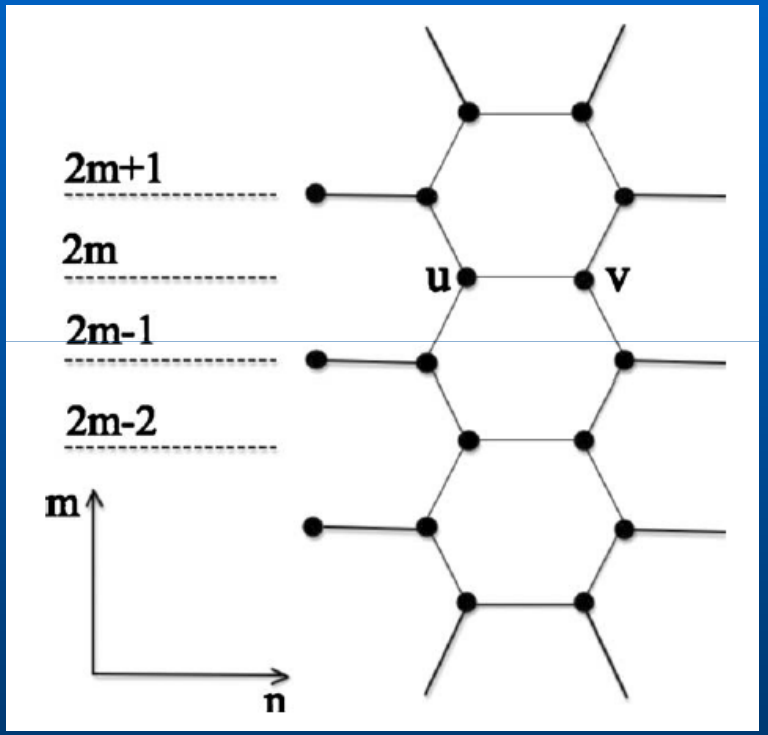

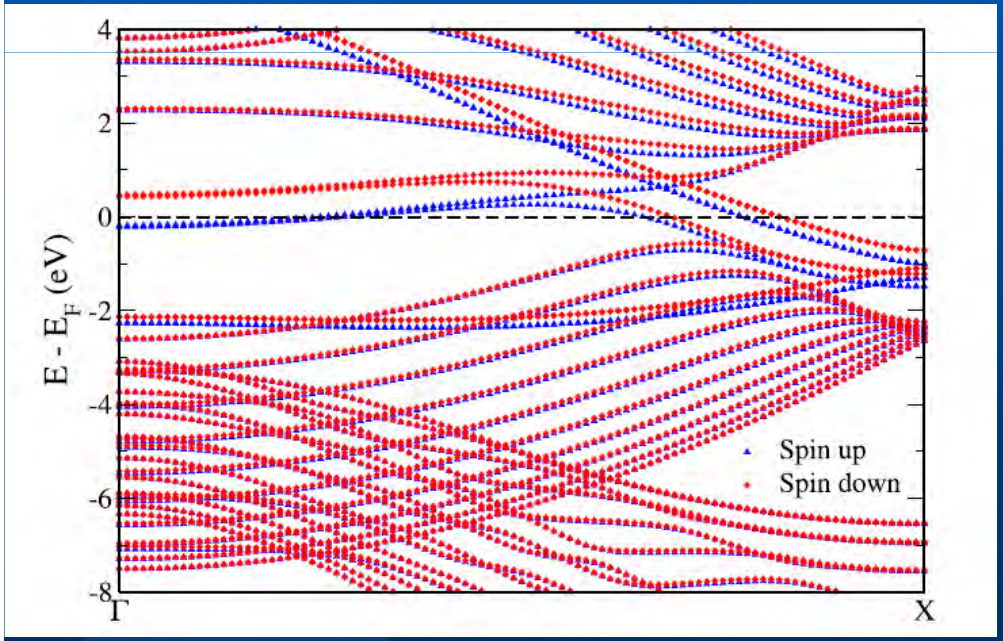

Zero-energy mode appears!

Spin-polarized bands in carbon-terminated nanoribbons

Dangling bonds in grain boundaries

Akhukov, Fasolino, Gornostyrev & MIK, PR B 85, 115407 (2012)

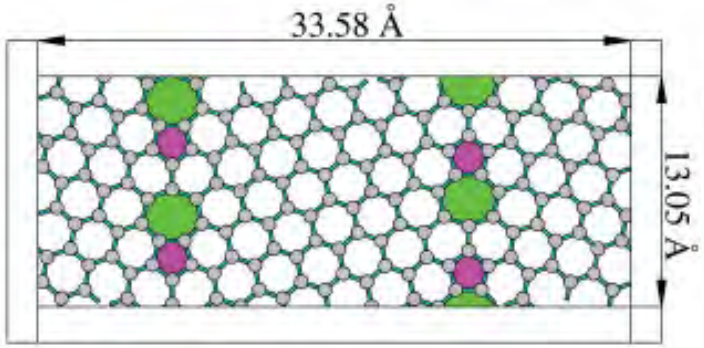

57 defect is nonmagnetic

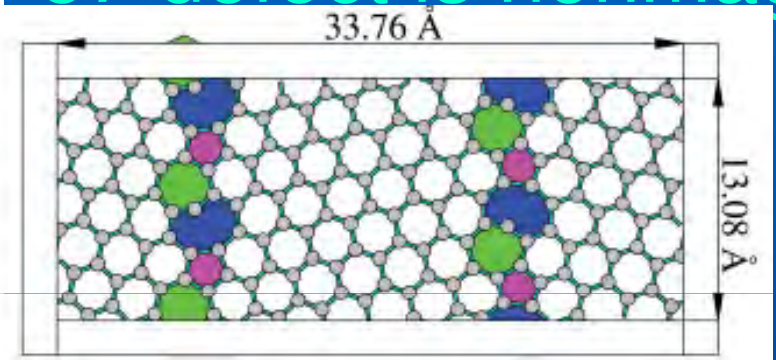

587 Magnetic and typical

And more...

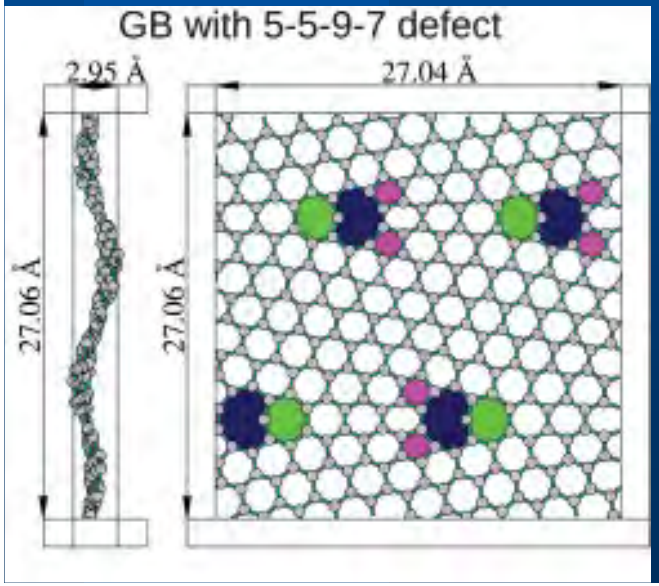

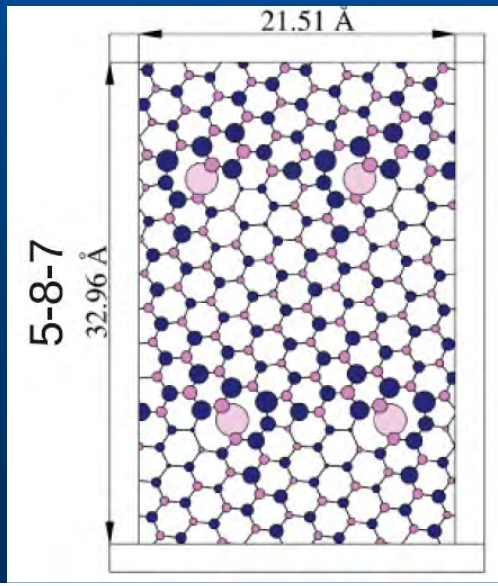

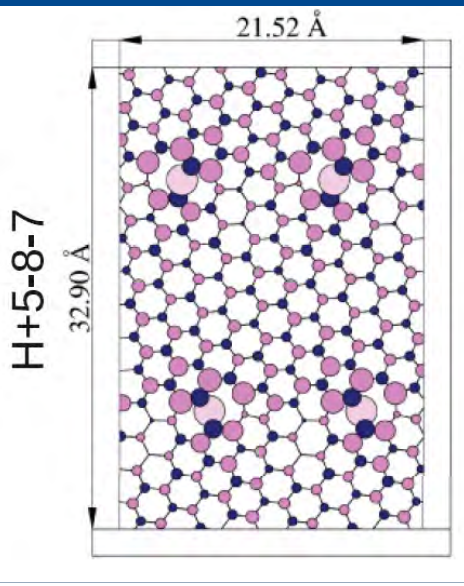

Spin density

Carbon foams

Akhukov, MIK & Fasolino, J. Phys.: Cond. Mat. 25, 255301 (2013)

24,000 configurations; about 1% have magnetic moments

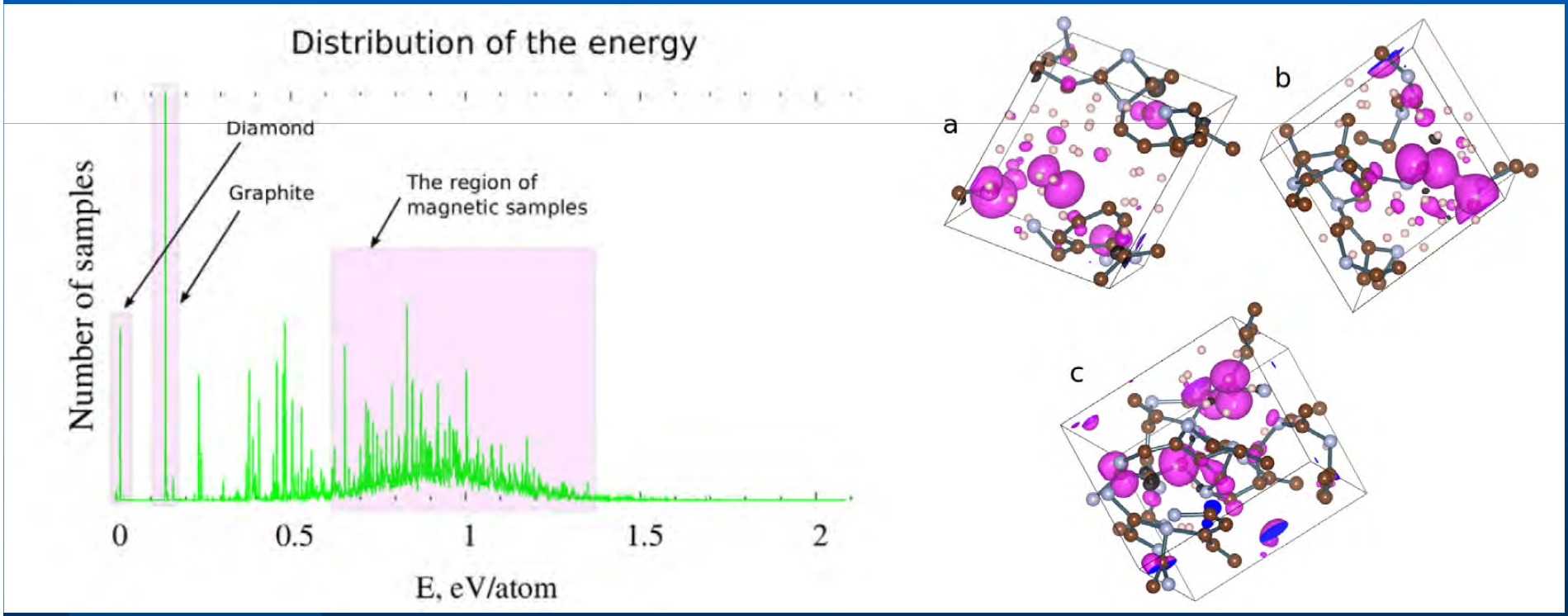

Nanotube-terminated nanoribbons

Akhukov, Yuan, Fasolino & MIK, New J. Phys. 14, 123012 (2012)

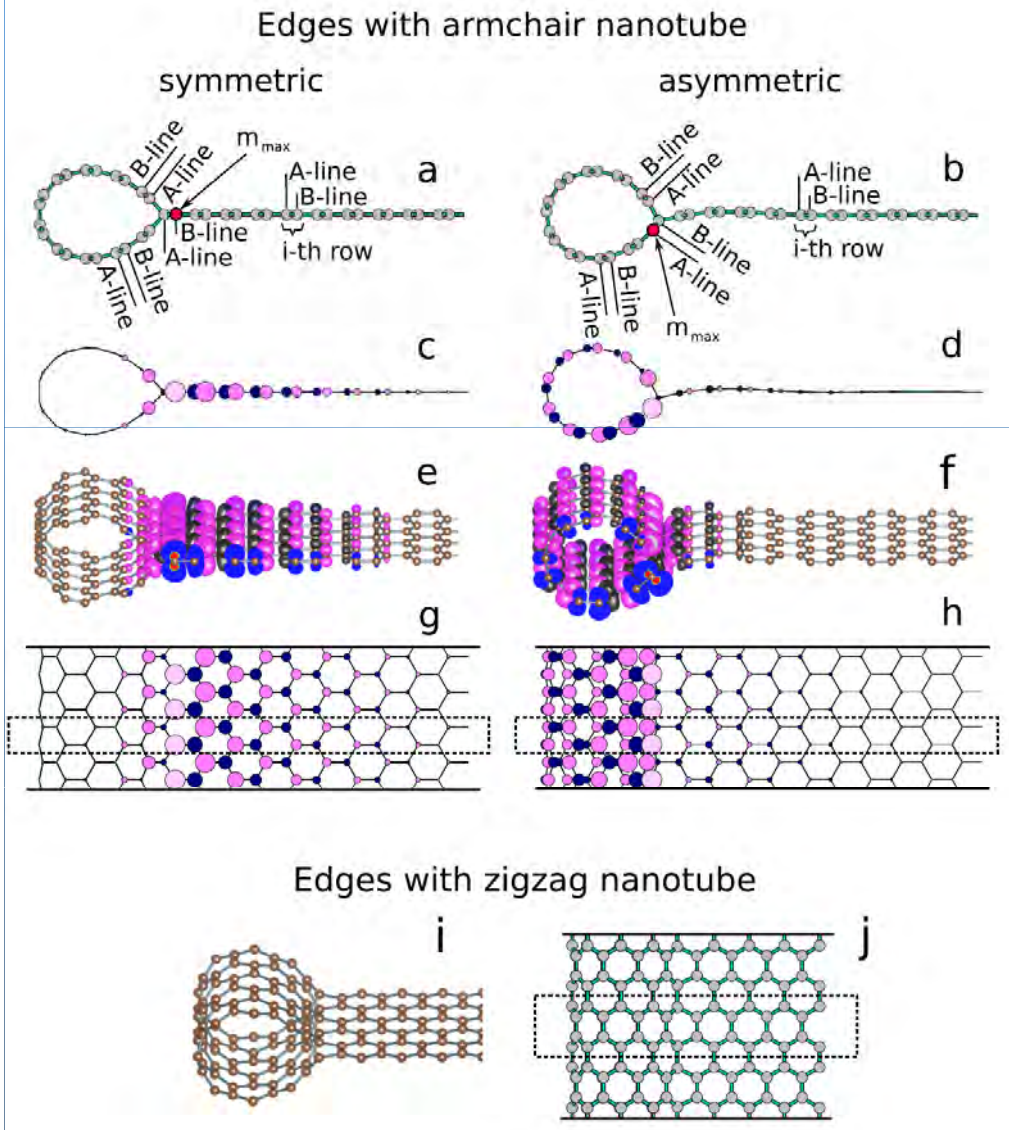

Figure 1. (a)–(h) Structure and spin density for symmetric (left) and asymmetric (right) AC nanotube terminated edges. (a), (b) Atomic structure; (c), (d) side, (e), (f) three-dimensional (3D) and (g), (h) top view of schematic spin representation. The box with a dashed line in (g), (h) indicates half of the unit cell in the density functional theory (DFT) calculation. For the symmetric case, the contribution to the magnetic moment from atoms belonging to the A- and B-sublattices are $m_A = 0.958\mu_B$ and $m_B = -0.217\mu_B$ (per half unit cell), and for the asymmetric case $m_A = 1.048\mu_B$ and $m_B = -0.300\mu_B$. The maximum of the magnetic moment is located on the atom indicated by the arrow with the value $m_{max} = 0.379\mu_B$ in both the symmetric and asymmetric cases. (i), (j) 3D and top view of AC nanoribbons terminated by ZZ nanotubes. The box with a dashed line in (j) indicates half of the unit cell in the DFT calculation.

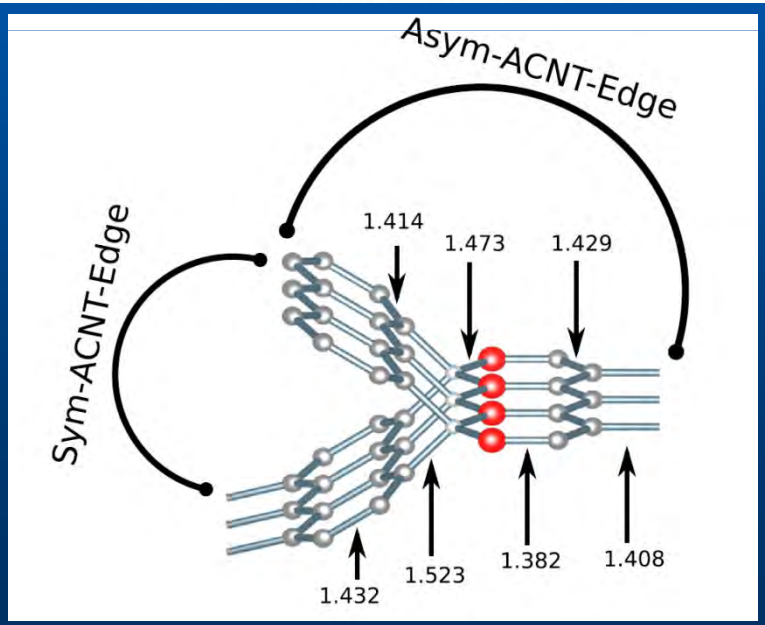

red = magnetic; sp^2-sp^3 bonds

Exchange interactions in concentrated systems

PHYSICAL REVIEW B **88**, 081405(R) (2013)

Exchange interactions and frustrated magnetism in single-side hydrogenated and fluorinated graphene

A. N. Rudenko,[1,*] F. J. Keil,[1] M. I. Katsnelson,[2] and A. I. Lichtenstein[3]

Two-side fluorinated or hydrogenated graphene is nonmagnetic. Single-side: claim for FM

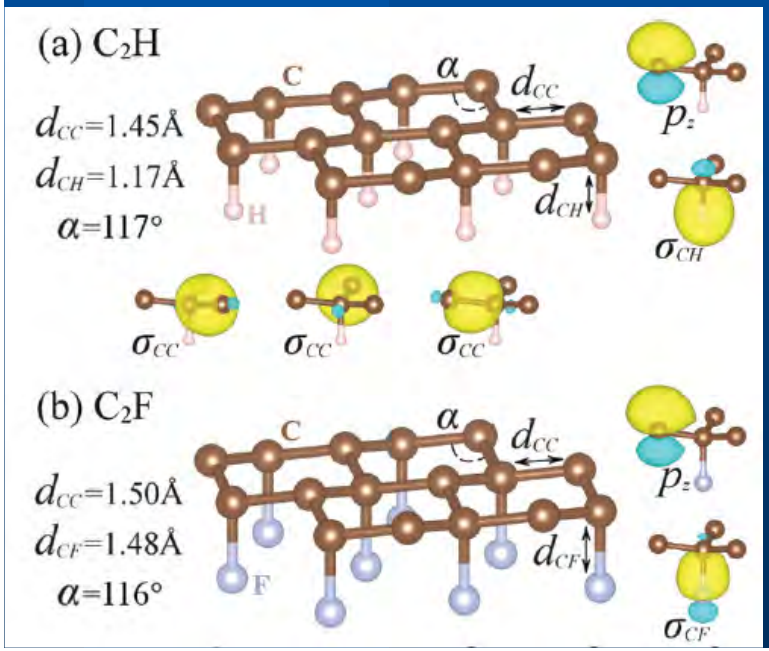

Structure, orbitals, nonmagnetic bands

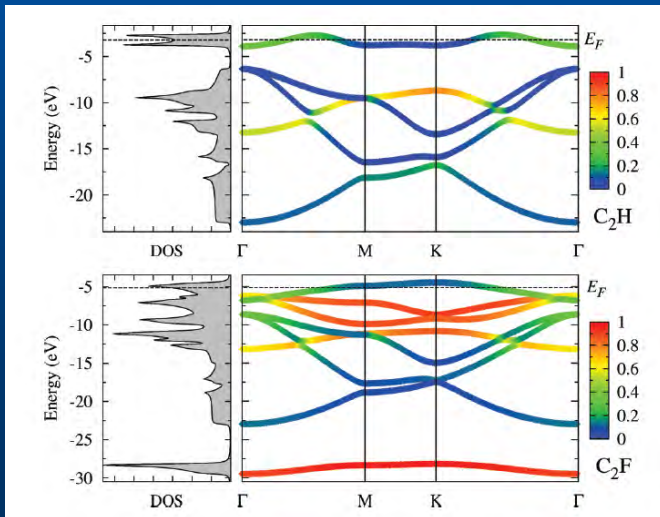

FIG. 2. (Color online) Band structure and density of states (DOS) for C_2H and C_2F obtained from non-spin-polarized calculations. Contributions from the impurity orbitals (*s* for H and *sp* for F) are shown by color.

Single-side C_2F and C_2H

Mapping on classical Heisenberg model (A. Lichtenstein & MIK)

$$H = -\sum_{i \neq j} J_{ij} \mathbf{s}_i \cdot \mathbf{s}_j$$

$$J_{ij}^{\alpha\beta} = \frac{1}{4\pi} \int_{-\infty}^{E_F} d\varepsilon \, \mathrm{Im}\left[\Delta_\alpha G_{ij}^{\alpha\beta\downarrow}(\varepsilon) \Delta_\beta G_{ji}^{\beta\alpha\uparrow}(\varepsilon)\right]$$

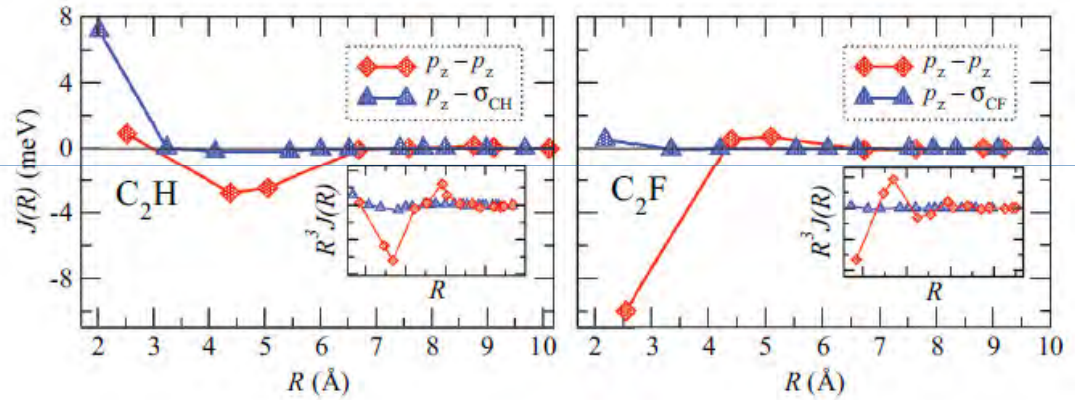

Well-localized magnetic moments

Quantum effects: Quantum spin liquid?!

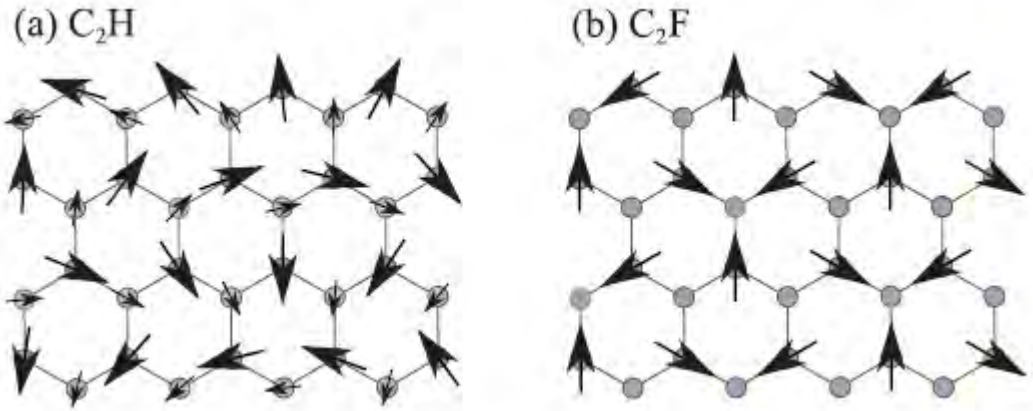

FIG. 5. (Color online) Spin structures corresponding to a classical ground state for (a) C_2H (incommensurate spin spiral) and (b) C_2F (120° Néel state).

Strength of Coulomb interactions in graphene

Wehling, Şaşıoğlu, Friedrich, Lichtenstein, MIK & Blügel, PRL106, 236805 (2011)

Generalized Hubbard model for π-bands only

$$\hat{H}_0 = -t \sum_{<\mathbf{i},\mathbf{j}>,\sigma} c^{\dagger}_{\mathbf{i},\sigma} c_{\mathbf{j},\sigma} - t' \sum_{\ll\mathbf{i},\mathbf{j}\gg,\sigma} c^{\dagger}_{\mathbf{i},\sigma} c_{\mathbf{j},\sigma}$$

$$+U_{00} \sum_{\mathbf{i}} n_{\mathbf{i},\uparrow} n_{\mathbf{i},\downarrow} + \frac{1}{2} \sum_{\mathbf{i}\neq\mathbf{j},\sigma,\sigma'} U_{\mathbf{ij}} n_{\mathbf{i},\sigma} n_{\mathbf{j},\sigma'}$$

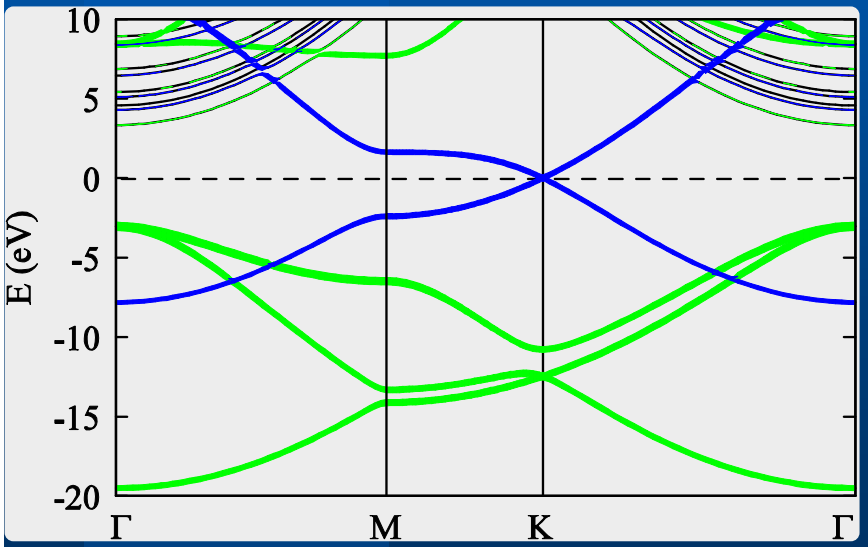

π bands (blue) crossing Fermi level

σ bands (green) at higher energies

All electrons except π contribute to screening of the Coulomb interactions (constrained RPA)

$$P(\mathbf{r},\mathbf{r}';\omega) = \sum_{i}^{\text{occ}} \sum_{j}^{\text{unocc}} \psi_i(\mathbf{r})\psi_i^*(\mathbf{r}')\psi_j^*(\mathbf{r})\psi_j(\mathbf{r}') \times \left\{ \frac{1}{\omega - \varepsilon_j + \varepsilon_i + i0^+} - \frac{1}{\omega + \varepsilon_j - \varepsilon_i - i0^+} \right\}$$

Polarization function

Strength of Coulomb interactions in graphene II

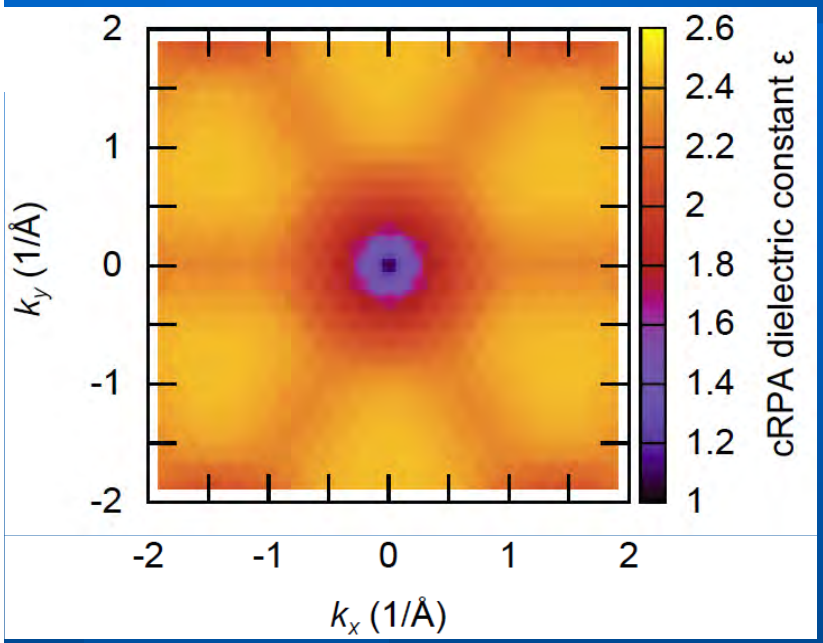

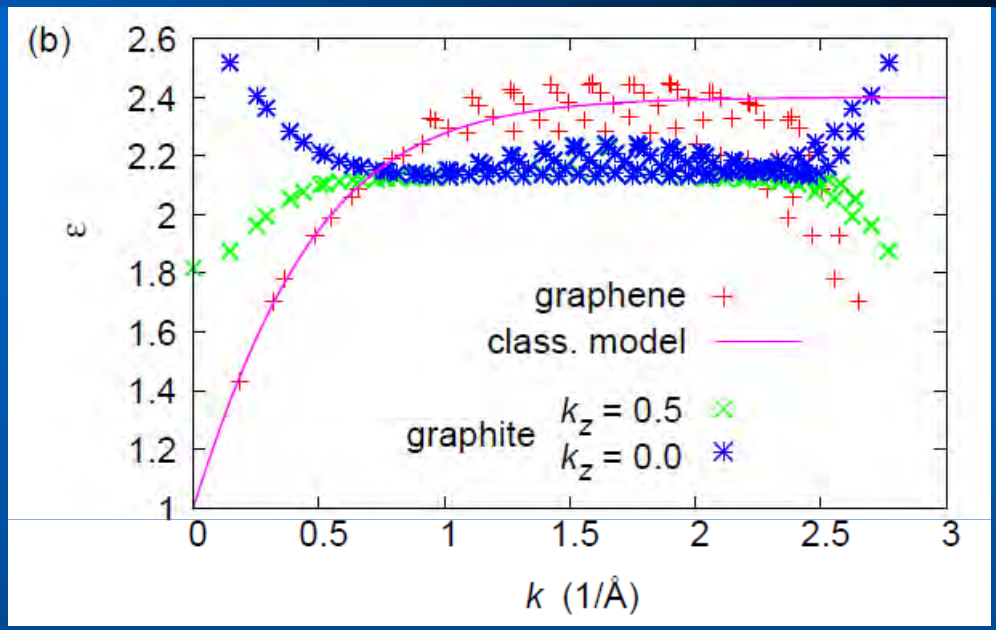

Static cRPA dielectric function of graphene in momentum space

Graphene vs graphite

	graphene		graphite	
	bare	cRPA	bare	cRPA
U_{00}^{A} (eV)	17.0	9.3	17.5	8.0
U_{00}^{B} (eV)	17.0	9.3	17.7	8.1
U_{01} (eV)	8.5	5.5	8.6	3.9

Strength of Coulomb interactions in graphene

	graphene		graphite	
	bare	cRPA	bare	cRPA
U_{00}^{A} (eV)	17.0	9.3	17.5	8.0
U_{00}^{B} (eV)	17.0	9.3	17.7	8.1
U_{01} (eV)	8.5	5.5	8	

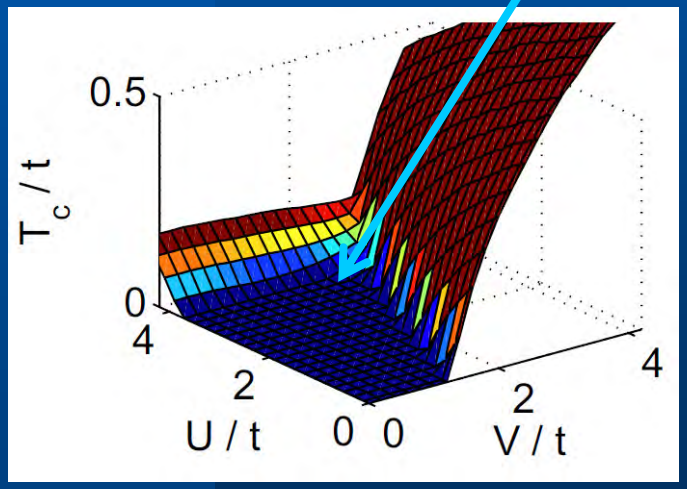

Honercamp, PRL 100, 146404 (2008)

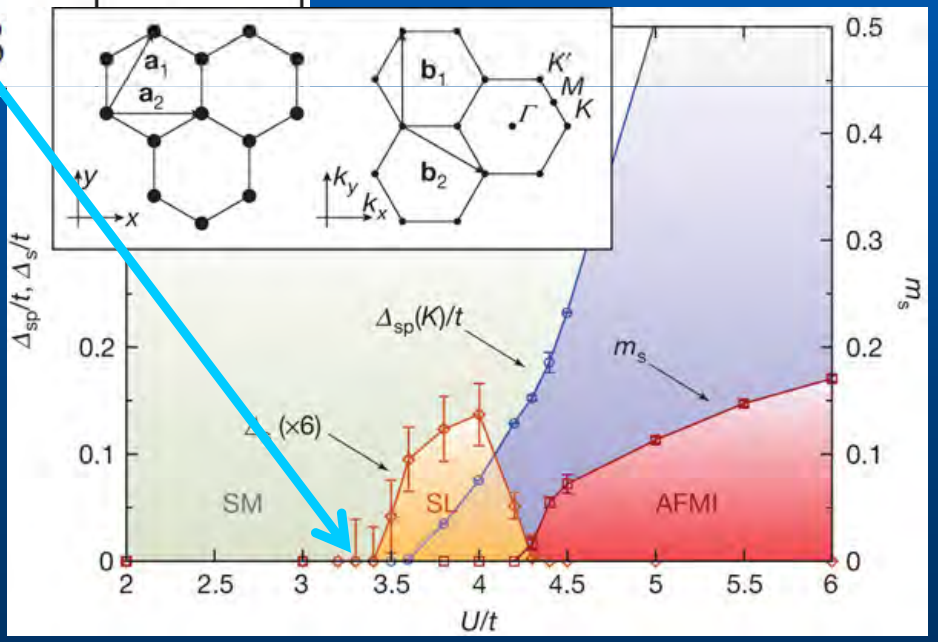

Z. Y. Meng et al., Nature **464**, 847 (2010)

Effect of strain on Coulomb interactions in graphene

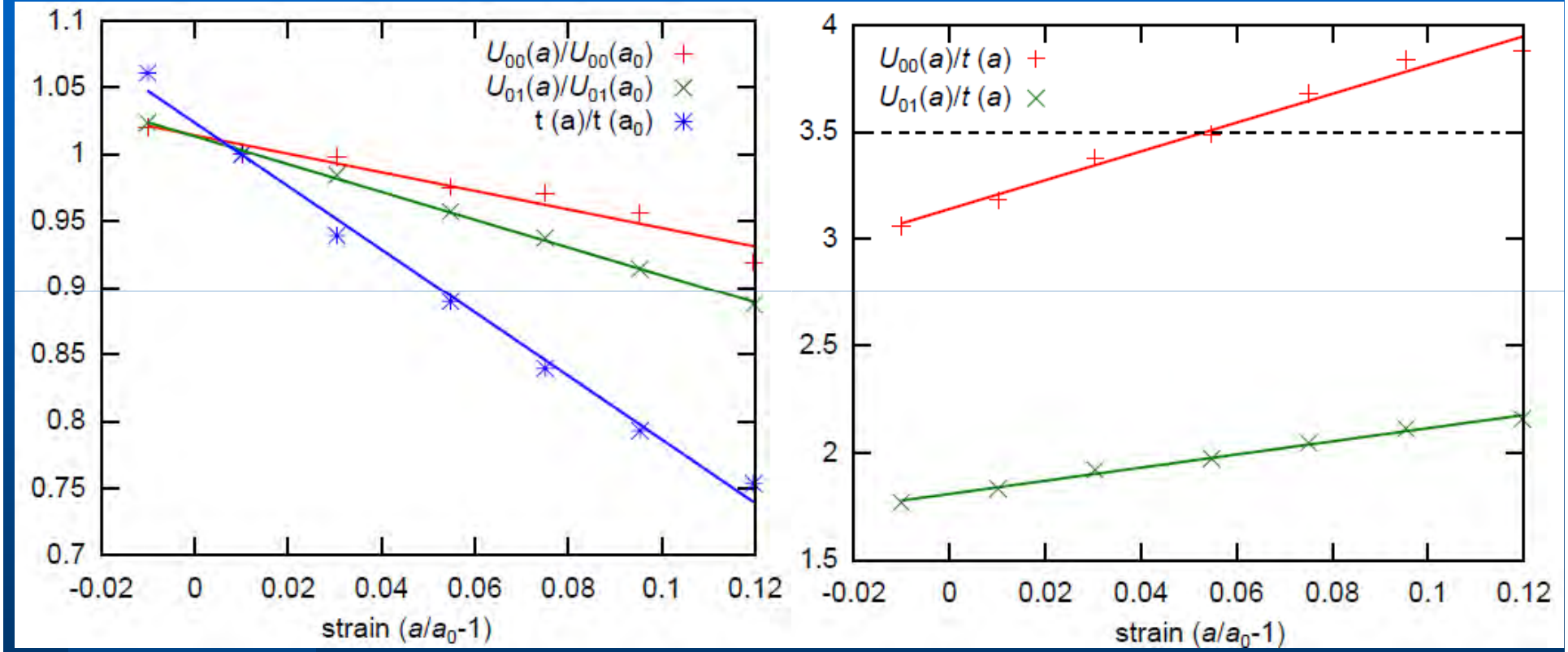

Coulomb interaction U_{ij} and hopping parameters t as function of lattice constant a.

The equilibrium lattice constant is a_0 = 2.47Å.

Semimetal-insulator phase transition

M. Ulybyshev, P. Buividovich, MIK & M. Polikarpov, PRL111, 056801 (2013)

Lattice QMC simulations; Hubbard-Stratonovich transformation:

18 by 18 sites,
20 time slices,
T = 0.5 eV

(should be improved in future!)

$$\exp\left(-\frac{\delta}{2}\sum_{x,y}\hat{q}_x V_{xy}\hat{q}_y\right) \cong$$

$$\cong \int \mathcal{D}\varphi_x \exp\left(-\frac{\delta}{2}\sum_{x,y}\varphi_x V^{-1}_{xy}\varphi_y - i\delta\sum_x \varphi_x \hat{q}_x\right),$$

$$\mathrm{Tr}\, e^{-\beta\hat{H}} = \int \mathcal{D}\varphi_{x,n}\mathcal{D}\psi_{x,n}\mathcal{D}\eta_{x,n}\mathcal{D}\bar{\psi}_{x,n}\mathcal{D}\eta_{x,n}$$

$$e^{-S[\varphi_{x,n}] - \sum\limits_{x,y,n,n'}\left(\bar{\eta}_{x,n}\bar{M}_{x,y,n,n'}\eta_{y,n'} + \bar{\psi}_{x,n}M_{x,y,n,n'}\psi_{y,n'}\right)},$$

$$\mathrm{Tr}\, e^{-\beta\hat{H}} \cong \int \mathcal{D}\varphi_{x,n} e^{-S[\varphi_{x,n}]} \left|\det\left(M\left[\varphi_{x,n}\right]\right)\right|^2$$

Neutrality point: μ = 0

No sign problem (e-h symmetry)!

$$S\left[\varphi_{x,n}\right] = \frac{\delta}{2}\sum_{x,y,n}\varphi_{x,n}V^{-1}_{xy}\varphi_{y,n}$$

Semimetal-insulator phase transition II

The effect of screening by σ-bonds is essential. At our distances a factor 1.4

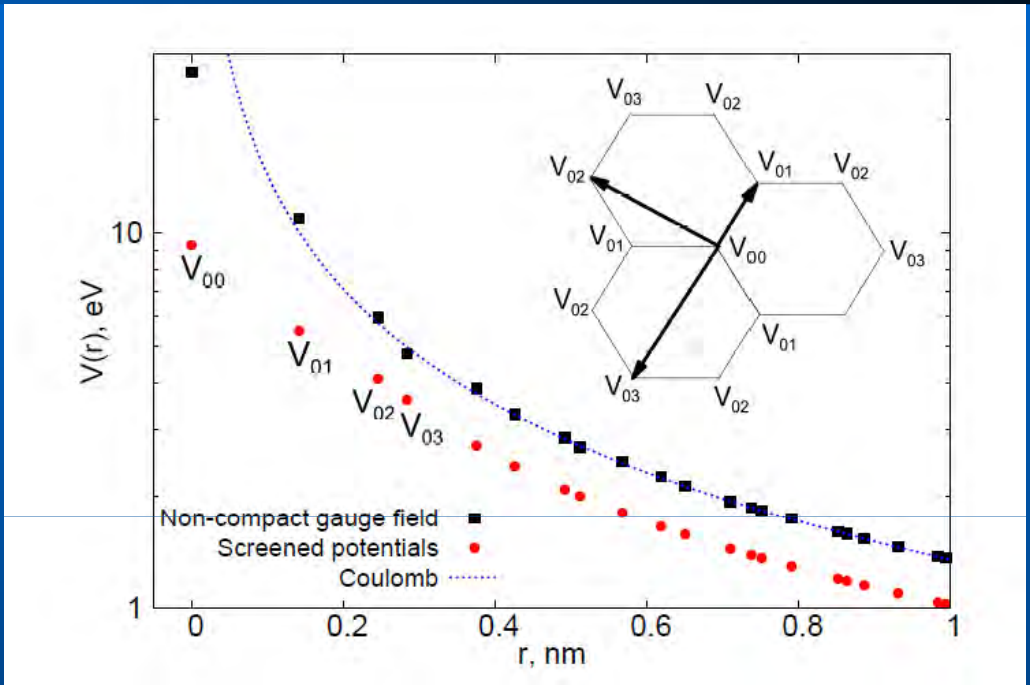

(1) Introduce the mass term *m*

(2) Chiral condensate Δ*n*, difference in occupation number between A and B sublattices

(3) Introduce external dielectric constant (due to substrate) ε

Semimetal-insulator phase transition III

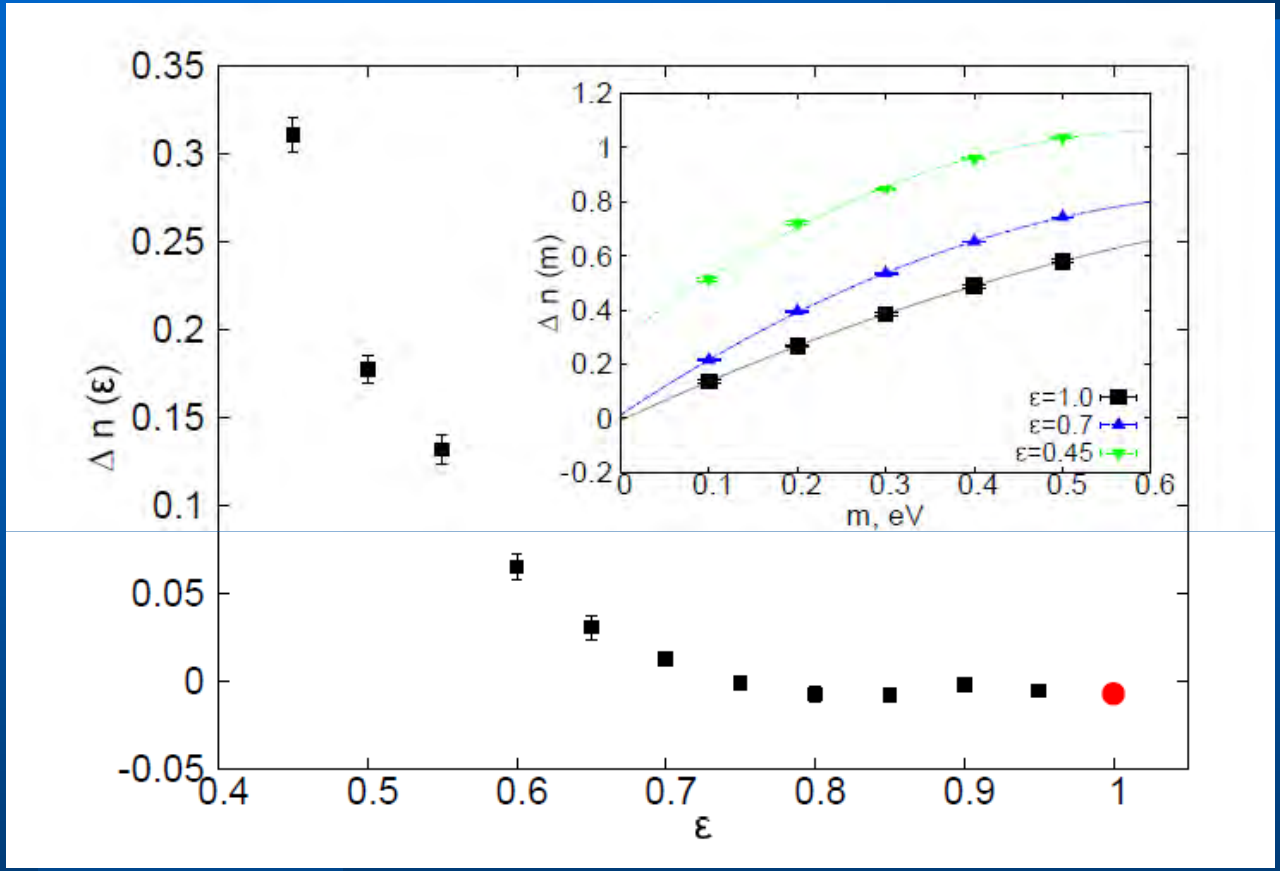

We are on semimetal side (screening by σ bonds is crucial) but not too far from the transition point $\varepsilon \approx 0.7$

Exciton fluctuations may be important

FIG. 2: The dependence of the chiral condensate (11) on ϵ and on m (in the inset) for the 18×18 lattice with $N_t = 20$ and $\delta = 0.1\,\mathrm{eV}^{-1}$. For $\epsilon = 1.0$ we show the results obtained on the 24×24 lattice with $N_t = 40$, $\delta = 0.05\,\mathrm{eV}^{-1}$.

Effective Hubbard model for graphene

Schűler, Rösner, Wehling, Lichtenstein & MIK, PRL 111, 036601 (2013)

Long-range Coulomb interection is crucially important for graphene but not everywhere, e.g., for magnetism effective Hubbard model should be OK. How to build it?

We have:

$$H = -\sum_{i,j,\sigma} t_{ij} c^{\dagger}_{i\sigma} c_{j\sigma} + U \sum_{i} n_{i\uparrow} n_{i\downarrow} + \frac{1}{2} \sum_{\substack{i \neq j \\ \sigma,\sigma'}} V_{ij} n_{i\sigma} n_{j\sigma'}$$

We want:

$$H^* = -\sum_{i,j,\sigma} t_{ij} c^{\dagger}_{i\sigma} c_{j\sigma} + U^* \sum_{i} n_{i\uparrow} n_{i\downarrow}$$

Effective Hubbard model for graphene II

The idea: Feynman-Peirels-Bogoliubov variational principle

$$\tilde{\Phi}[\rho^*] = \Phi^* + \langle H - H^* \rangle^*$$

$$\Phi^* = -\frac{1}{\beta} \ln Z^*$$

$$\rho^* = 1/Z^* e^{-\beta H^*}$$

$$Z^* = \mathrm{Tr}\left\{ e^{-\beta H^*} \right\}$$

$\langle \dots \rangle^*$ denotes the Gibbs average over the trial system

$$\partial_{U^*} \tilde{\Phi}[U^*] = 0$$

$$U^* = U + \frac{1}{2} \sum_{\substack{i \neq j \\ \sigma, \sigma'}} V_{ij} \frac{\partial_{U^*} \langle n_{i\sigma} n_{j\sigma'} \rangle^*}{\sum_l \partial_{U^*} \langle n_{l\uparrow} n_{l\downarrow} \rangle^*}$$

The calculations are done by lattice QMC

Effective Hubbard model for graphene III

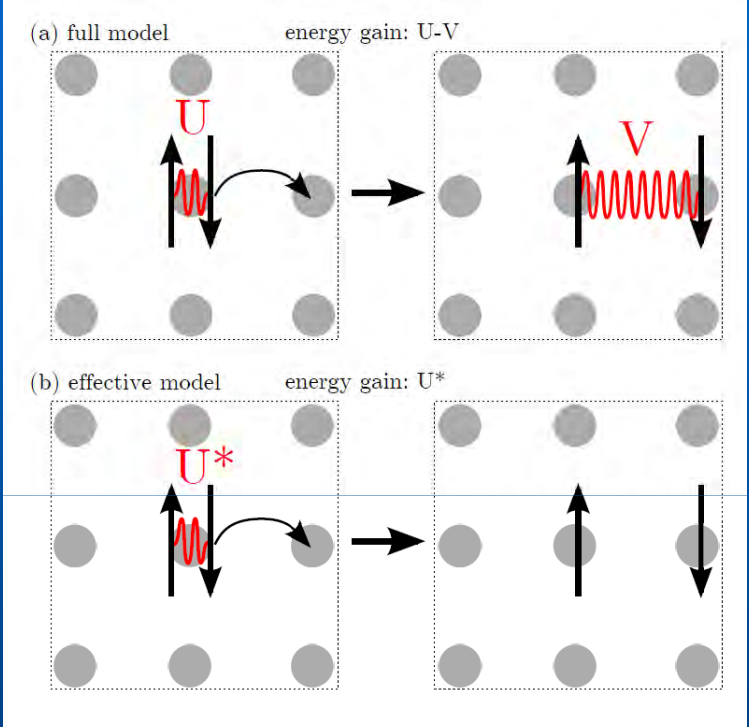

For translationally invariant system:

$$U^* = U - \bar{V}$$

$$\bar{V} = -\sum_{\substack{j\neq 0 \\ \sigma'}} V_{0j} \frac{\partial_{U^*} \langle n_{0\uparrow} n_{j\sigma'} \rangle^*}{\partial_{U^*} \langle n_{0\uparrow} n_{0\downarrow} \rangle^*}$$

Number of particle conservation

$$\sum_{j\sigma} \langle n_{0\uparrow} n_{j\sigma} \rangle^* = N/2$$

$$\partial_{U^*} \langle n_{0\uparrow} n_{0\downarrow} \rangle^* = -\sum_{j\neq 0,\sigma} \partial_{U^*} \langle n_{0\uparrow} n_{j\sigma} \rangle^*$$

A naive estimation: $U^* = U - V_{01}$

turns out to be amazingly good

Effective Hubbard model for graphene IV

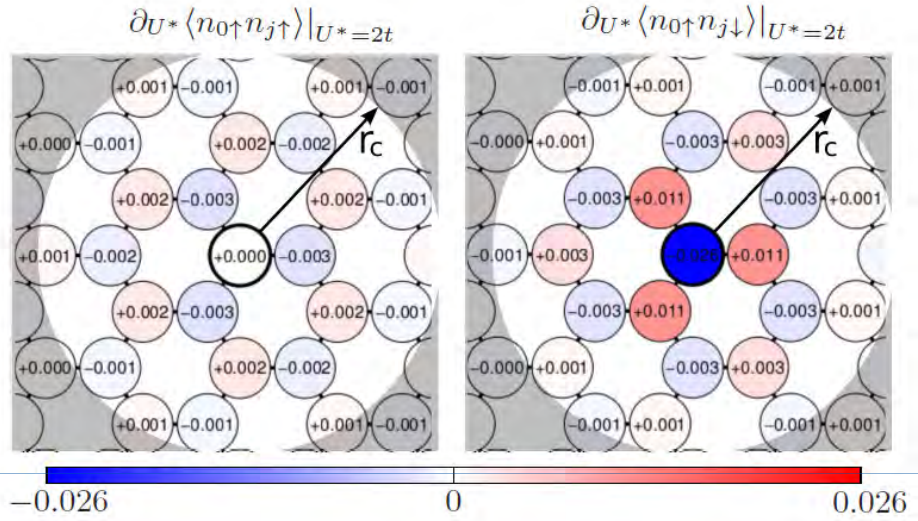

Figure 2. (Color online) Derivatives of the correlation functions $\langle n_{0\uparrow}n_{j\sigma}\rangle$ with respect to U^* for graphene (16x16 unit cells) calculated with DQMC for inverse temperature $\beta = 9t$ and $U = 2t$. Each circle corresponds to one carbon atom. The shaded area depicts the region of nearly vanishing derivatives. The cutoff radius is r_c. The thick drawn circles indicate the lattice site with index $i = 0$.

Calculations for benzene, graphene and silicene

Table I. First three rows: Coulomb matrix elements obtained with cRPA ($t_{\text{graphene}} = 2.80$ eV, $t_{\text{silicene}} = 1.14$ eV, $t_{\text{benzene}} = 2.54$ eV). Last three rows: Effective local Coulomb matrix elements with and without the approximation that electrons are only displaced to next neighbors and the factor by which the local Coulomb interaction is decreased.

	Graphene	Silicene	Benzene
U/t	3.63	4.19	3.96
$(V_{01},V_{02})/t$	2.03,1.45	2.31,1.72	2.83,2.01
$(V_{03},V_{04})/t$	1.32,1.14	1.55,1.42	1.80
U^*/t	1.6 ± 0.2	2.0 ± 0.3	1.2
$(U - V_{01})/t$	1.6	1.9	1.1
U^*/U	0.45 ± 0.05	0.46 ± 0.05	0.3

Decrease of effective *U* roughly by a factor of 2

Conclusions

- sp electron magnetic semiconductors can be better than conventional – if one finds FM...
- local magnetic moments is not a problem but FM is; even when one has strong exchange it is not necessarily FM
- very unclear situation for magnetism at the edges (beyond the talk)
- for theoretical studies one can use Hubbard model with first-principles Hubbbard parameter; Intersite Coulomb interaction decrease it roughly by a factor of 2

Main collaborators

M.Akhukov, A.Fasolino, A.Rudenko (Nijmegen)
A.Geim, I.Grigorieva, K.Novoselov (Manchester)
D.Edwards (Imperial, London)
O. Yazyev (Lausanne)
A.Lichtenstein (Hamburg)
T.Wehling (Bremen)
M.Polikarpov (Moscow)
D.Boukhvalov (Seoul)
O.Eriksson (Uppsala)

MANY THANKS!